International Journal of Electrical, Electronic and Communication Sciences
ISSN: 2517-9438
Vol:3, No:8, 2009

# Electrical Performance of a Solid Oxide Fuel Cell Unit with Non-Uniform Inlet Flow and High Fuel Utilization

Ping Yuan, Mu-Sheng Chiang, Syu-Fang Liu, Shih-Bin Wang, and Ming-Jun Kuo

***Abstract*—**This study investigates the electrical performance of a planar solid oxide fuel cell unit with cross-flow configuration when the fuel utilization gets higher and the fuel inlet flow are non-uniform. A software package in this study solves two-dimensional, simultaneous, partial differential equations of mass, energy, and electro-chemistry, without considering stack direction variation. The results show that the fuel utilization increases with a decrease in the molar flow rate, and the average current density decreases when the molar flow rate drops. In addition, non-uniform Pattern A will induce more severe happening of non-reaction area in the corner of the fuel exit and the air inlet. This non-reaction area deteriorates the average current density and then deteriorates the electrical performance to –7%.

***Keywords*—**Performance, Solid oxide fuel cell, non-uniform, fuel utilization.

## I. Introduction

A solid oxide fuel cell (SOFC) has been identified as a technology for the high-efficiency conversion of hydrocarbon fuels to electric energy, and environmentally friendly power generation. The electrolyte of SOFC is made of solid materials, typically nickel/zirconia cermet, so it has higher reliability than other kinds of fuel cells. Solid oxide fuel cells operate at high temperatures of about 600-1000°C, and use methane or ethanol as fuel due to internal self-reformation. The high temperature exhaust heat obtained simultaneously with power generation is used in fuel reforming, bottoming power generation, and the regenerative heating of fuel and air, as a result of which the total power generation efficiency of the entire cycle is high. Given a cell geometry, the performance of a SOFC strongly depends on the operating conditions and the fuel utilization. The planar-type solid oxide fuel cell stacks easily and is desirable for many applications. Several recent studies investigated performance simulation under different conditions, since fuel rate, inlet temperature, operation pressure, cell size, etc. affect temperature and current density distribution.

Achenbach [1] presented a three-dimensional simulation for the gas, current density, and temperature distribution of a planar solid oxide fuel cell, which accounts for time-dependent effect, flow configurations, internal methane-steam reforming, and recycling of the anode gas. Recknagle et al. [2] simulated a three-dimensional SOFC unit with three kinds of flow patterns using the same commercial package for reaction area performance. The authors showed temperature, current density, and fuel composition distribution with three flow configurations, i.e. co-flow, counter-flow, and cross-flow. Beale et al. [3] investigated three different numerical method approaches for solving a unit and a ten-stack SOFC with cross-flow. Results indicated that the direct numerical method is the most accurate single cell method. Simpler approaches can potentially supplant or complement the direct numerical method in fuel cell stack analysis. Iwata et al. [4] established a numerical program to estimate temperature and current density profiles of a planar-type SOFC unit with co-flow, counter-flow, and cross-flow. That study investigated gas re-circulation ratio, operating pressure, and physical property effects on current and temperature distributions. The above literature used numerical method to solve the temperature and current density distribution on the reaction area, but all of them consider the inlet flow of the fuel and air is uniform on the frontal area. Recently, Yuan and Liu [5] investigated the temperature and current density distributions in a SOFC unit when the inlet flows of the anode gas and the cathode gas are mal-distributed in eight patterns. The results showed that the non-uniform inlet flow of fuel and air affect the current density distribution and temperature distribution, respectively.

Fuel utilization is a key factor, because it represents an economical operation of a fuel cell when the fuel utilization is higher. The normal fuel utilization of a SOFC is close to 50%, and the fuel utilization of previous literature is between 50% and 70%. Au et al [6] executed a project of operation of a high-temperature SOFC using mine gas, and presented results of the mine gas analyses and their effect on the pre-reformer and the fuel cell in the fuel utilization of 50% and 70%. Based on the saving energy source concept, most fuel cell operates in high fuel utilization in order to reduce the waste of hydrogen. Araki et al [7] combined four stages SOFC to promote the total fuel utilization to be 99.98% after the fourth stage. However,

P. Yuan is with the Lee Ming Institute of Technology, Taipei 24305, Taiwan, ROC (phone: 886-2-29097811; fax: 886-2-229095888; e-mail: pyuan@mail.lit.edu.tw).

M.S. Chiang is with the Nan Kai University of Technology, Nantou 54243, Taiwan, ROC. (e-mail: sam@nkut.edu.tw).

S. F. Liu is with Lee Ming Institute of Technology, Taipei 24305, Taiwan, ROC (e-mail: sfl@mail.lit.edu.tw).

S.B. Wang is with with Lee Ming Institute of Technology, Taipei 24305, Taiwan, ROC (e-mail: wsb@mail.lit.edu.tw).

M.J. Kuo is with with Lee Ming Institute of Technology, Taipei 24305, Taiwan, ROC (e-mail: mjkuo@mail.lit.edu.tw).

all performance analysis of a SOFC unit in above literature is under a condition of uniform inlet flow on the frontal area, except the literature by us. Because the fuel molar flow rate dominantly affects the current density of a fuel cell, the non-uniform inlet flow effect must induce an appearance of non-reaction on the cell plane when the fuel utilization is high. This non-reaction area also decreases the overall current density of a cell and deteriorates the electrical performance of a solid oxide fuel cell. Therefore, this paper plans to extend previous research to the current density distribution analysis of a solid oxide fuel cell when the fuel inlet flow is non-uniform and the fuel utilization gets higher.

## II. Analysis

In order to compare the effect of non-uniform inlet fuel flow rate on the performance of a SOFC unit in different sizes, this study analyze the current density and temperature distribution on a reaction area of $0.2\times0.2$ standing for the laboratory scale. The fuel flows in the x direction, and the air flows in the y direction, as shown in Fig. 1. For simplifying analysis, this study combines the anode, electrolyte, and cathode to form a unit, which is named of the cell in this study. In Fig. 1, the inlet flow distribution along the transverse direction may be a progressive decreasing or progressive increasing profile, but not a uniform profile perfectly, because of the fuel inlet duct position being near either the air inlet or air exit side. According to the results of Yuan and Liu [5], the fuel and air molar flow rate dominantly affects the current density and the cell temperature, respectively. Therefore, this paper considers the air inlet is uniform and the fuel inlet has three profiles, as shown in Fig. 2. Meanwhile, the character d represents non-uniform profile deviation, and it is below 0.5 for most cases in practical application. Before formulating the governing equations, this study assumes: 1.) Inlet temperature and mole fractions of species in fuel and air are constant and uniform. 2.) Thermal properties of fuel, air, cell, and inter-connector are constant except for fuel and air specific heat capacities. 3.) Cell and inter-connector boundary are adiabatic. 4.) Neglect z direction change. 5.) Cell voltage is uniform over the x-y plane. 6.) Neglect the water-shift reaction in the fuel.

The chemistry reaction in both anode and cathode side are as follows.

$$CO + O^{2-} \rightarrow CO_2 + 2e^- \quad (1)$$

$$H_2 + O^{2-} \rightarrow H_2O + 2e^- \quad (2)$$

$$O_2 + 4e^- \rightarrow 2O^{2-} \quad (3)$$

Meanwhile, Eq. (1) and (2) occurs in anode, and the electrochemical oxidation rate of hydrogen is about two times higher than that of carbon monoxide reported by Matsuzaki and Yasuda[8]. It means that the hydrogen consumption rate is double of carbon monoxide consumption rate.

Mass balances are formulated for each species molar flow rate change in fuel and air with species consumption linking the local current density. Due to this study considers the reformed methane or ethanol in the external reformer and the reforming gases are fed into the SOFC, the feed fuel includes hydrogen ($H_2$), nitrogen ($N_2$), carbon dioxide ($CO_2$), carbon monoxide (CO), and water ($H_2O$). In cathode, the air is fed into the SOFC, so the species only includes the oxygen and nitrogen.

$$\frac{1}{L_y}\frac{d\left(n_f X_j\right)}{dx} = \pm\frac{i}{2F} \quad (4)$$

$$\frac{1}{L_x}\frac{d\left(n_a X_j\right)}{dy} = -\frac{i}{4F} \quad (5)$$

Meanwhile, $n$ is the molar flow rate, $X_j$ is the mole fraction of j-component, and the plus/minus symbol represents molar flow rate increase or decrease dependent on reactant or product species.

This research conserves energy for fuel, air, cell, and inter-connector, respectively.

For fuel,

$$\frac{d}{dx}\left(\sum n_f X_j c_{p,j} T_f\right) = (ha)_{i-f}\left(T_i - T_f\right) + (ha)_{c-f}\left(T_c - T_f\right) + \frac{i}{4F} c_{p,O_3^{2-}} T_c \quad (6)$$

For air,

$$\frac{d}{dy}\left(\sum n_a X_j c_{p,j} T_a\right) = (ha)_{i-a}\left(T_i - T_a\right) + (ha)_{c-a}\left(T_c - T_a\right) - \frac{i}{4F} c_{p,O_3^{2-}} T_a \quad (7)$$

For cell,

$$-(k\delta)_c \frac{\partial^2 T_c}{\partial x^2} - (k\delta)_c \frac{\partial^2 T_c}{\partial y^2} = (ka)_{i-c}\frac{\left(T_i - T_c\right)}{\delta_{i-c}} + (ka)_{i-c}\frac{\left(T_i - T_c\right)}{\delta_{i-c}} + (ha)_{c-f}\left(T_f - T_c\right) + (ha)_{c-a}\left(T_a - T_c\right) + \frac{i}{4F} c_{p,O_3^{2-}} T_a - \frac{i}{4F} c_{p,O_3^{2-}} T_c + \dot{q}_{reac} \quad (8)$$

For inter-connector,

$$-(k\delta)_i \frac{\partial^2 T_i}{\partial x^2} - (k\delta)_i \frac{\partial^2 T_i}{\partial y^2} = (ka)_{i-c}\frac{\left(T_c - T_i\right)}{\delta_{i-c}} + (ka)_{i-c}\frac{\left(T_c - T_i\right)}{\delta_{i-c}} + (ha)_{i-f}\left(T_f - T_i\right) + (ha)_{i-a}\left(T_a - T_i\right) \quad (9)$$

Each gas species specific heat capacities in fuel and air are a function of temperature, and this study selects half of oxygen specific heat capacity as oxygen ion specific heat capacity. In Eq. (6) to (8), the term $ic_{p,O^{2-}}T/4F$ describes heat transfer rate as oxygen ion migrates from the air side to the fuel side through the cell. In Eq. (8) and (9), $k_{ci}$ is thermal conductivity due to contact resistance between cell and inter-connector in the z direction, and its value is set to 1.0 W/m K. Additionally, $q_{reac}$ in Eq. (8) is heat generation occurring in the cell unit due to electrochemical reactions and cell internal losses, and this heat generation occurs over the x-y plane as follows.

$$\dot{q}_{rect} = -\Delta H \times \frac{i}{2F} - V \cdot i \quad (10)$$

$$\Delta H = -240506 - 7.3835 T_c \quad (11)$$

Based on the Nernst equation, this study calculates the Nernst voltage as follows.

$$E = E_0 + \frac{RT}{2F}\ln\left(\frac{P_{H_2} P_{O_2}^{0.5}}{P_{H_2O}}\right) \quad (12)$$

$$E_0 = 1.2723 - 2.7654\times10^{-4} T_c \quad (13)$$

Meanwhile, $E_0$ is the reversible voltage under standard conditions. The difference between the Nernst voltage and the cell voltage represents the voltage loss, which contains ohmic loss, electrode activation loss, and concentration loss.

$$E - V = V_{ohm} + V_{act} + V_{con} \quad (14)$$

Because concentration loss in the cathode is less than that in the anode when the SOFC cell is electrolyte-supported and anode-supported, this study neglects concentration loss in the cathode based on the results of Chan et al. [9]. Therefore, cell voltage is equal to the Nernst voltage by subtracting the loss of ohmic, activation, and concentration in anode as follows.

$$V_{ohm} = ir \tag{15}$$

$$V_{act} = \frac{RT}{2F}\sinh^{-1}\left(\frac{i}{2i_{0,anode}}\right) + \frac{RT}{2F}\sinh^{-1}\left(\frac{i}{2i_{0,cathode}}\right) \tag{16}$$

$$V_{con} = -\frac{RT}{2F}\ln\left[\frac{1-(RT/2F)(\delta_{anode}/D_{anode}p_{H_2})\cdot i}{1+(RT/2F)(\delta_{anode}/D_{anode}p_{H_2O})\cdot i}\right] \tag{17}$$

Here, $r$ is $300\times10^{-7}\Omega/m^2$, $i_{0,anode}$ and $i_{0,cathode}$ are 1290 and 970 A/m$^2$, respectively, the $\delta_{anode}$ is 0.05mm, and $D_{anode}$ is $2\times10^{-5}$ m/s.

This study utilizes a software package, FlexPDE to solve six unknown variables in the governing equations when the cell voltage is set to be a constant. These variables include mole fractions of each species in both fuel and air, the temperature of fuel, air, inter-connector, and cell, as well as current density. The validation of this software package had done in the literature by Yuan and Liu [5]. Because this paper considers the situation of a SOFC in the high fuel utilization, some reaction area maybe lack hydrogen due to the nonuniform fuel mole flow profile. In the calculation process, the software code judges the pressure of hydrogen in Eq. (17) whether it is equal to or smaller than zero. If the judgment is validated, the program code neglects the calculation of all polarizations and sets them to be zero in Eq. (14), which induces the zero current density in Eq. (15).

## III. Results and Discussion

This study considers the fuel flow rate is 0.00225-0.009 mol/s, the air flow rate is 0.009 mol/s, the inlet temperature of fuel and air are both 898 K, the operation pressure is 1 atm, the operation voltage is 0.7 V, and the deviation of the non-uniform profile is 0.5. Fig. 3 shows that the current density distribution in Pattern A and Pattern B when the fuel and air flow rate is 0.0045 and 0.009 mol/s, respectively. In this figure, the profile in bold line is the current density distribution in the condition of uniform pattern, and the profile in color represents current density distribution in Pattern A or Pattern B. Examining the current density distribution in uniform pattern indicates that the current density mainly decreases along the fuel flow direction from 7050 to 2760 A/m$^2$. In the air flow direction, the current density slightly drops because of the decrease of oxygen concentration. In Fig. 3(a), the current density of Pattern A has more severe reduction in the corner of the fuel exit and the air inlet. In this corner, the hydrogen concentration becomes lower because the progressively increasing fuel profile induces less fuel flowing through this area. Oppositely, the area with apparent current drop happens in the corner of the fuel exit and the air exit in Fig. 3(b), because the fuel non-uniform profile is progressively decreasing in Pattern B. Comparing the Fig. 3(a) and 3(b) indicates that the current density drop in the corner of Fig. 3(a) is larger than that of Fig. 3(b), and even the current density drops to zero in Fig. 3(a). In Fig. 3, the fuel utilization in uniform, Pattern A, and Pattern B is 74.3, 70.9, and 72.6%, respectively. It is obvious that the uniform profile has the largest fuel utilization, and both Pattern A and B has lesser utilization. Because there is a non reaction area in Pattern A, it has the lower fuel utilization than Pattern B. Therefore, Pattern B is better than Pattern A, if the uniform profile is out of consideration.

Fig. 4 shows that the current density distribution in Pattern A and Pattern B when the fuel and air flow rate is 0.00338 and 0.009 mol/s, respectively. In this figure, the profile with bold line is the current density distribution in uniform pattern, and the profile with color represents current density distribution in Pattern A or Pattern B. Examining the current density distribution in uniform pattern indicates that the current density mainly decreases along the fuel flow direction from 7020 to 920 A/m$^2$. This current density range is clearly lower than that in Fig. 3. Because the fuel molar flow rate is smaller than that in Fig. 3, the current density becomes lower due to the less hydrogen concentration. In Fig. 4(a), the current density has a dramatic reduction in the corner of the fuel exit and the air inlet. In this corner, the current density rapidly decreases from 3000 A/m$^2$ to zero. This means the region is non-reaction area. The less fuel flow rate and non-uniform inlet flow profile induces the fuel molar flow rate is fewer in this area, so the hydrogen is used out and the current density becomes zero. In pattern B, although the current density severely drops in the corner of the fuel exit and the air exit in Fig. 4(b), the non-reaction area is smaller than that in Fig. 4(a). Because the fuel consumption near the air exit is originally less than that near the air inlet when the inlet flow is uniform liking in bold line, the reduced inlet fuel flow due to the non-uniform profile still can supply the reaction till nearing its exit.

Fig. 5 shows that the current density distribution in Pattern A and Pattern B when the fuel and air flow rate is 0.00225 and 0.009 mol/s, respectively. The non-reaction area of Fig. 5(a) is apparently larger than that of Fig. 4(a), because the fuel molar flow rate is the least in this study. Even in uniform pattern, the current density distribution happen a severe drop in the corner of the fuel exit and the air inlet, as shown in the bold line. This means the fuel is already used out in this portion when the fuel flows out the fuel cell reacting area when the inlet flow is uniform. Examining the current density change shows that it is between 0 to 7000 A/m$^2$, which is the lowest one in Figs. 3 to 5. In Fig. 5(b), the current density in the corner of the fuel exit and the air exit also drops to zero because of the decreasing overall fuel inlet molar flow rate.

Promoting the fuel utilization in a fuel cell is an important factor based on the economical viewpoint, but the global current density will drop with a rapid decreasing in hydrogen concentration and then induces the power decrease of a fuel cell. Moreover, the non-reaction area will happen when the fuel inlet molar flow rate becomes less or the fuel inlet profile is non-uniform, which more deteriorates the global current density. Table I lists the average current density and fuel utilization in all cases of this study at 0.7 voltage. In this table, it is clear that the average current density and fuel utilization decreases and increases with a decrease in the molar flow rate, respectively. Furthermore, Pattern A has the lowest average current density and fuel utilization comparing to the results in uniform and Pattern B, because Pattern A induces the severe happening of non-reaction area in the corner of the fuel exit and the air exit.

Fig. 6 depict the histogram of relative change of average current density in non-uniform pattern related to that in uniform pattern. In this figure, the relative change is close to –4% and

-2% in Pattern A and B, respectively, when the fuel molar flow rate is 0.0045 mol/s. The minus represents the average current density becomes lower when the inlet profile is non-uniform. Once the fuel molar flow rate decreases, the fuel utilization will increase but the effect of non-uniform inlet flow on the average current density becomes more apparent when the fuel utilization gets higher. In this figure, the relative change of average current density raise up to –7% in Pattern A when the inlet molar flow rate of the fuel is 0.00338 mol/s. In this situation, the non-reaction area happens and the deterioration of electrical performance due to the non-uniform inlet flow cannot be neglected.

## IV. Conclusion

This study investigates the effect of non-uniform inlet flow on the electrical performance of a SOFC unit. This work employed a software package to solve the simultaneous mass equations, energy equations, and electrochemistry equations. With considering three flow patterns and different fuel molar flow rates, this research analyzed the current density distributions at different conditions. The results show that the fuel utilization and average current density increases and decreases with a decrease in the fuel molar flow rate, respectively. In addition, non-uniform Pattern A will induce a severe happening of non-reaction area in the corner of the fuel exit and the air inlet comparing to Pattern B did. This non-reaction area deteriorates the average current density and deteriorates the electrical performance to –7% when the fuel molar flow rate is 0.00338 mol/s and fuel utilization is 83.3%. This study suggests that the fuel inlet manifold should be located far from the inlet of air, which will decrease the deterioration due to non-uniform profile below -3%.

## Acknowledgement

This study was supported by the National Science Council, the Republic of China, through grant number NSC 96-2221-E-234-002.

TABLE I
Average Current Density and Fuel Utilization at Different Inlet Molar Flow Rate and Patterns

| Case/ Flow rate (mol/s) | Uniform | | Pattern A | | Pattern B | |
|---|---|---|---|---|---|---|
| | $i$ (A/m$^2$) | $U_f$ (%) | $i$ (A/m$^2$) | $U_f$ (%) | $i$ (A/m$^2$) | $U_f$ (%) |
| Case 1 $n_f$ =9E-3 | 5080 | 43.3 | 5027 | 42.8 | 5033 | 42.9 |
| Case 2 $n_f$ =7.88E-3 | 4947 | 48.2 | 4891 | 47.6 | 4895 | 47.7 |
| Case 3 $n_f$ =6.75E-3 | 4793 | 54.5 | 4727 | 53.7 | 4731 | 53.8 |
| Case 4 $n_f$ =5.63E-3 | 4605 | 62.8 | 4490 | 61.2 | 4535 | 61.8 |
| Case 5 $n_f$ =4.5E-3 | 4360 | 74.3 | 4161 | 70.9 | 4260 | 72.6 |
| Case 6 $n_f$ =3.38E-3 | 3953 | 89.8 | 3664 | 83.3 | 3835 | 87.2 |

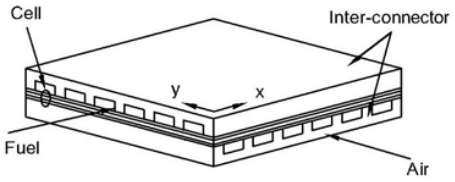


Fig. 1 Schematic diagram of a unit of solid oxide fuel cell in cross-flow

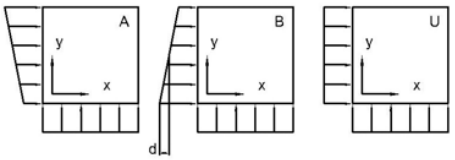


Fig. 2 Arrangements of non-uniform inlet flow patterns in this study

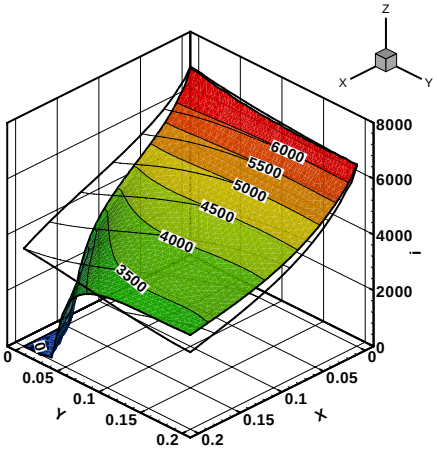


(a) Pattern A

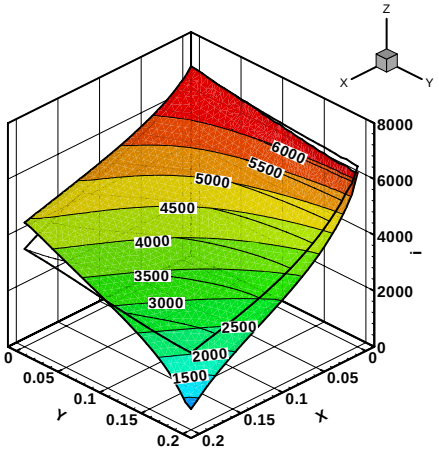


(b) Pattern B

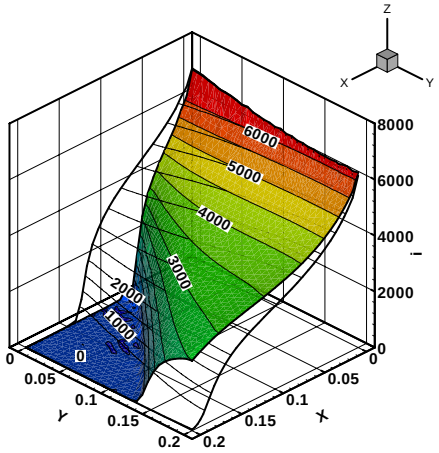


(a) Pattern A

Fig. 3 Current density distribution when $n_f$ =0.0045

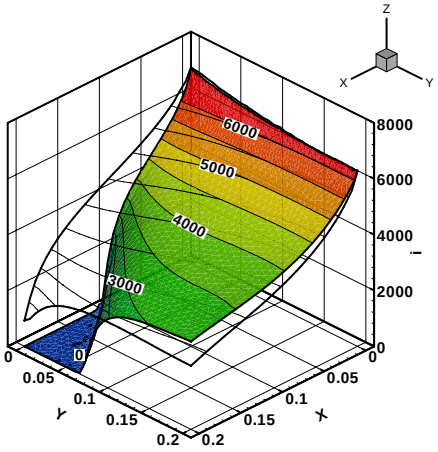


(a) Pattern A

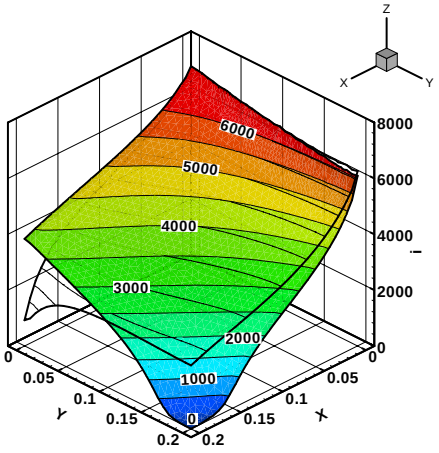


(b) Pattern B

Fig. 4 Current density distribution when $n_f$ =0.00338

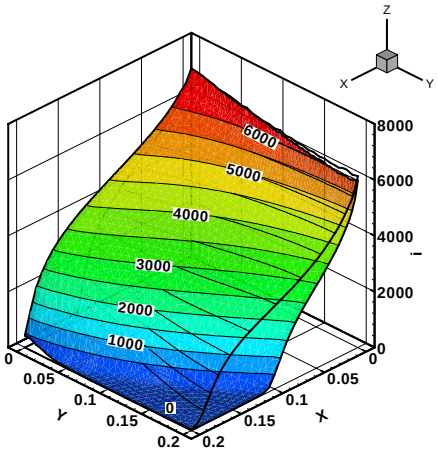


(b) Pattern B

Fig. 5 Current density distribution when $n_f$ =0.00225

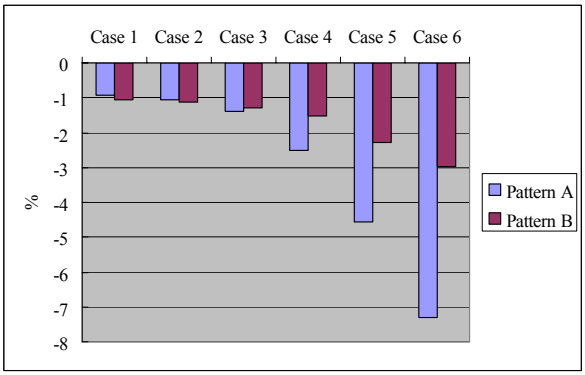


Fig. 6 Relative change of average current density in non-uniform pattern related to a uniform pattern

## REFERENCES

[1] Achenbach, E., "Three-dimensional and time-dependent simulation of a planar solid oxide fuel cell stack". J. Power Sources, vol. 49, pp. 333-348, 1994.
[2] Recknagle, K.P., Williford, R.E., Chick, L.A., Rector, D.R., Khaleel, M.A., "Three-dimensional thermo-fluid electrochemical modeling of planar SOFC stacks". J. Power Sources, vol. 113, pp. 109-114, 2003.
[3] Beale, S.B., Lin, Y., Zhubrin, S.V., Dong, W., "Computer methods for performance prediction in fuel cells" J. Power Sources, vol. 118, pp. 79-85, 2003.
[4] Iwata, M., Hikosaka, T., Morita, M., Iwanari, T., Ito, K., Onda, K., Esaki, Y., Sakaki, Y., Nagata, S., "Performance analysis of planar-type unit SOFC considering current and temperature distributions". Solid State Ionics, vol. 132, pp. 297-308, 20000.
[5] Yuan, P., Liu, S.F., "Numerical Analysis of Temperature and Current Density Distribution of a Planar Solid Oxide Fuel Cell Unit with Non-uniform Inlet Flow". Numerical Heat Transfer, Part A, vol. 51 pp. 941-957, 2007.
[6] Au, S.F., Blum, L., Dengel, A., Grob, B., de Haart, L.G.J., Kimmerle, K., Wolf, M., "Utilization of mine gas with a high-temperature SOFC fuel cell". Journal of Power Sources, vol. 145, pp. 582-587, 2005.
[7] Araki, T., Taniuchi, T., Sunakawa, D., Nagahama, M., Onda, K., Kato, T., "Cycle analysis of low and high $H_2$ utilization SOFC/gas turbine combined cycle for $CO_2$ recovery". Journal of Power Sources, vol. 171, pp. 464-470, 2007.
[8] Matsuzaki, Y., Yasuda, I., "Electrochemical oxidation of $H_2$ and CO in a $H_2$- $H_2O$-CO-$CO_2$ system at the interface of a Ni-YSZ cermet electrode and YSZ electrolyte". J. Electrochem. Soc., vol. 147, pp. 1630-1635, 2000.
[9] Chan, S.H., Khor, K.A., Xia, Z.T., "A complete polarization model of a solid oxide fuel cell and its sensitivity to the change of cell component thickness". J. Power Sources, vol. 93, pp. 130-140, 2001.